International Journal of Environmental Sciences
ISSN: 2229-7359
Vol. 11 No. 14s,2025
https://theaspd.com/index.php

Chitosan-Lignin-IM Nanocomposites for Efficient Removal of Cd(II) and Pb(II): Synthesis, Characterization, and Adsorptive Behavior

Hussein Sadiq Khashan[1], Tayseer Shamran Al-Deresawi[2]
[1,2] Department of Biology, College of Education for Pure Sciences, University of Wasit, Al-Kut City, Iraq.
[1]asdfg0yrgjr@gmail.com ,[2]tshamran@uowasit.edu.iq

Abstract
Heavy metals like cadmium (Cd^{2+}) and lead (Pb^{2+}) can contaminate water and cause serious health risks. They also harm the environment. This study focused on making and testing a new nanocomposite called Chitosan-Lignin-IM. It was made by crosslinking chitosan with glutaraldehyde. Lignin was added next, followed by conjugation with 4-carboxylic imidazole using EDC/NHS. The structure and chemistry of the material were confirmed using FESEM and FT-IR. FESEM showed a uniform nanostructure. FT-IR confirmed the bonding of the functional groups. Adsorption tests showed high efficiency at pH 6–7. Over 90% of both Cd^{2+} and Pb^{2+} were removed at this range. The maximum adsorption was 142 mg/g for cadmium and 165 mg/g for lead. The material followed time-dependent uptake. It reached equilibrium in 2 to 3 hours. Swelling tests showed steady water absorption. The maximum swelling degree reached 467% after 5 hours. Viscosity tests showed shear-thinning behavior. This means it can flow easily under stress. The results show that the nanocomposite is efficient, fast, and stable in water. Its performance is better than many traditional materials. The addition of imidazole helped improve both metal binding and dispersion. This makes the material suitable for safe and practical water treatment.
Keywords: *Adsorption, Cadmium, Chitosan, Lignin, Nanocomposites*

INTRODUCTION

Clean water is becoming harder to find. Heavy metals are one of the main reasons. Pollutants like cadmium, lead, and mercury come from factories, farms, and sewage. These metals are toxic. They stay in the environment and build up in human and animal bodies. Even small amounts can cause serious damage. Removing them from water is difficult. Many existing methods are expensive or not very effective (1–3).

Because of this, researchers are exploring natural materials. Chitosan and lignin are two popular options. Chitosan comes from shellfish waste. It has many amino and hydroxyl groups. These can bind to metal ions. Lignin is a plant-based material. It has aromatic structures and reactive sites. This makes it useful for trapping pollutants (2,3).

Combining these two materials forms nanocomposites. These composites have better properties. They have more surface area and more active sites. This increases their ability to capture metals. Adding groups like imidazole can improve the material even more. Imidazole groups help bind metal ions. They also improve the dispersibility and flexibility of the material. Studies show that these modified composites can remove various heavy metals. They also work under different environmental conditions (1,4,6).

Lignin and chitosan composites are stable and easy to process. They are biodegradable and low-cost. They can also be adjusted for different pollutants. Some studies show they are good at removing dyes, oil, and drug residues (7–9). Recent research focuses on improving pore size, surface charge, and structure. Adding nanoparticles or functional groups helps. These changes make the materials more effective and stable in real-world water treatment (10–15). This study follows that approach. It develops a new Chitosan-Lignin-IM composite to remove Cd^{2+} and Pb^{2+}. The results support its use in environmental cleanup.

MATERIALS AND METHODS

Chitosan-Lignin Nanocomposite Synthesis The process started by preparing a 5% (w/v) chitosan solution. This was done by dissolving 500 mg of chitosan in 100 mL of distilled water. Separately, 1 mL of glutaraldehyde was acidified with acetic acid to reach a pH between 3 and 5. This step was important to

control the reaction speed and ensure uniform cross-linking. The acidified glutaraldehyde was then added dropwise to the chitosan solution while stirring constantly. Stirring was maintained at 1000 rpm using a mechanical stirrer for 3 hours. This allowed the cross-linking to spread evenly throughout the solution. In the second stage, lignin was added. A 0.25% (w/v) lignin solution was made by dissolving 250 mg of lignin in distilled water. This lignin solution was slowly poured into the chitosan-glutaraldehyde mixture under vigorous stirring. Stirring continued for 4 hours at room temperature. This helped blend the lignin into the chitosan matrix and form stable molecular bonds. The mixture turned thick and brown, showing good mixing. The final solution was poured onto glass dishes to form films. These dishes were degassed to remove any trapped air bubbles. The films were then dried in an oven at 37°C. This allowed the water to evaporate without damaging the polymers. The dried films were about 1 mm thick. They were smooth, flexible, and ready for chemical modification.

Preparation of Carboxylic Imidazole-Conjugated Chitosan-Lignin Nanocomposite

To functionalize the composite, a 100 mg/mL solution of 4-carboxylic imidazole (IM) was prepared. To this, 200 mg of EDC and 160 mg of NHS were added. These agents helped activate the carboxylic group in IM. The solution's pH was adjusted to 8–9 using 2N NaOH. The mixture was stirred at 80°C for 4 hours. This step ensured full activation before conjugation. The activated IM solution was then added slowly to the chitosan-lignin mixture. The entire solution was stirred under the same conditions and kept for 24 hours. This allowed enough time for the imidazole group to bind to the amino groups in chitosan. After the reaction, the product was identified as Chitosan-Lignin-IM.

To purify the final nanocomposite, the solution was placed into a 12 kDa dialysis bag. Dialysis was done in distilled water to remove excess chemicals. The material inside the bag was then dried. This gave the final Chitosan-Lignin-IM product in solid form. Its appearance changed after drying, showing successful modification.

Characterization of the Nanocomposites

FESEM was used to study the surface and structure of the composite. The sample was coated with a thin layer of platinum to make it conductive. Imaging was done using a MIRA TESCAN system from the Czech Republic. The voltage was set to 15 kV, and images were captured at 100,000× magnification. The particle shape and size were examined. The elemental content was also checked using energy-dispersive spectroscopy (EDS).

FT-IR spectroscopy was used to confirm the chemical bonds. A Tensor 2 (Bruker, Germany) instrument was used. Samples were mixed with 200 mg of KBr and pressed into pellets using a 12-ton press. Spectra were recorded between 400 and 4000 cm^{-1}. Peaks were analyzed to detect –OH, $–NH_2$, and imidazole groups. These signals confirmed the chemical changes in each step of the process.

The combined data from FESEM, EDS, and FT-IR gave a full picture of the nanocomposite. The surface images showed even distribution. The element mapping matched expected results. The FT-IR peaks confirmed that bonding had taken place. All three tools confirmed the success of the synthesis.

Cadmium and Lead Adsorption by Chitosan-Lignin-IM Nanocomposites

To test how well the composite removed cadmium and lead, solutions were prepared. Each metal solution had a concentration of 100 mg/L. For each test, 0.1 g of Chitosan-Lignin-IM nanocomposite was used. The pH of each solution was adjusted using either HCl or NaOH. Values tested were pH 2, 4, 5, 6, 7, 8, and 10. A digital pH meter was used for accuracy.

Each test was done in a beaker with 100 mL of the metal solution. The nanocomposite was added and the mixture was shaken at 150 rpm for 60 minutes. The temperature was kept at 25 ± 2°C. After mixing, the solution was filtered using Whatman No. 1 filter paper. The filtrate was collected for metal concentration testing.

An Atomic Absorption Spectrophotometer (AAS) was used to measure the remaining cadmium and lead in the solution. The adsorption capacity (qe, in mg/g) was calculated using a standard equation. This formula

used the starting and ending metal concentrations (C_0 and Ce), the volume of solution (V), and the weight of the nanocomposite (m). This method helped find the best pH for metal removal.

Effect of Incubation Time and Initial Concentration

To study how time and concentration affected adsorption, three metal concentrations were tested: 50, 100, and 200 mg/L. Each test used 0.1 g of the nanocomposite in 100 mL of solution. The experiments were done in 250 mL Erlenmeyer flasks. The mixtures were shaken at 150 rpm at 25 ± 2°C.The contact times tested were 0, 0.5, 1, 1.5, 2, 3, and 4 hours. At each time point, the mixture was filtered to remove the nanocomposite. The remaining metal concentration in the filtrate was measured using AAS. The same equation used in the pH study was applied to calculate qe.Results showed that metal adsorption increased with time. Most of the metal was removed in the first 2 to 3 hours. Higher initial metal concentrations led to higher adsorption capacity. These tests helped confirm how quickly the nanocomposite could work under different conditions.

Swelling Behavior of Chitosan-Lignin-IM Nanocomposites

To test how much water the composite could absorb, dried samples were weighed and placed in phosphate-buffered saline (PBS). The pH was 7.4 and the temperature was kept at 37°C. These conditions mimic the human body. Samples were taken out at different times: 0.5, 1.5, 3, 4, and 5 hours.

At each time point, excess liquid was removed using soft tissue. The wet sample was weighed. Then it was placed back into the PBS to continue swelling. The swelling degree (SD) was calculated using the formula:

SD = ((Ws − Wd) / Wd) × 100, where Ws is the swollen weight and Wd is the dry weight.

The swelling increased over time. At 5 hours, the swelling reached its highest point, 467%. This showed that the material could absorb a lot of water and expand. It also confirmed that the composite had a porous structure.

Evaluation of Viscosity of Chitosan-Lignin-IM Nanocomposites

To study the flow behavior, a rotational rheometer was used. The model was Anton Paar MCR 302 from Austria. A parallel plate geometry was used with a 25 mm diameter and 1 mm gap. The nanocomposite was first dispersed in deionized water. It was stirred for 24 hours to make sure it was fully hydrated and even

Tests were done at 25 ± 0.1°C. The shear rate was changed from 0.1 to 1000 s^{-1}. The apparent viscosity was recorded at each point. The results were shown on a log–log graph of viscosity versus shear rate. The curve showed that viscosity decreased as shear rate increase, This shear-thinning behavior means the material flows more easily when under force. This is helpful for processing and applying the material in real use. It supports the idea that the nanocomposite is stable, flexible, and suitable for water treatment systems.

RESULTS

Morphology and Structural Characterization

The morphology of the synthesized Chitosan-Lignin-IM nanocomposites was examined using Field Emission Scanning Electron Microscopy (FESEM). The micrograph in Figure 1 reveals a relatively uniform surface with spherical nanoparticle-like structures distributed across the matrix. These features suggest successful nanoparticle formation and structural homogeneity. Some surface roughness and textural variations are visible, indicating the presence of lignin and imidazole-modified domains within the chitosan framework. Elemental mapping by EDS (data not shown) confirmed the expected composition, supporting that the blending and conjugation steps did not disrupt the overall material integrity.

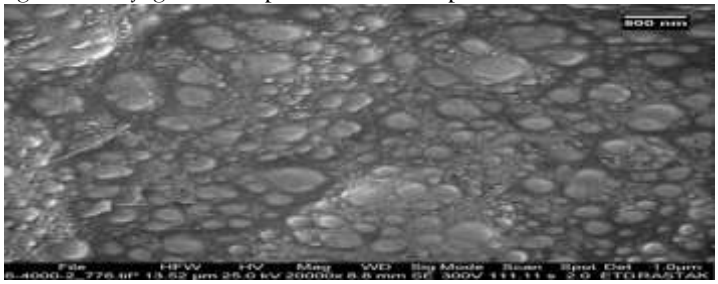

International Journal of Environmental Sciences
ISSN: 2229-7359
Vol. 11 No. 14s,2025
https://theaspd.com/index.php

Figure 1: FESEM image showing the surface morphology of Chitosan-Lignin-IM nanocomposite at high magnification. Nanostructures appear evenly distributed, indicating good integration of all components.

The particle size distribution of the composite is shown in Figure 2. The graph demonstrates a relatively narrow range of particle sizes, with the majority falling below 100 nm, confirming nanoscale characteristics. Such small sizes are advantageous for enhancing surface area and active site availability, which are essential for adsorption processes. This observation aligns with prior expectations regarding chitosan-lignin hybrids and their efficiency in forming compact structures. The results provide initial confirmation of successful synthesis and support the composite's suitability for adsorption experiments.

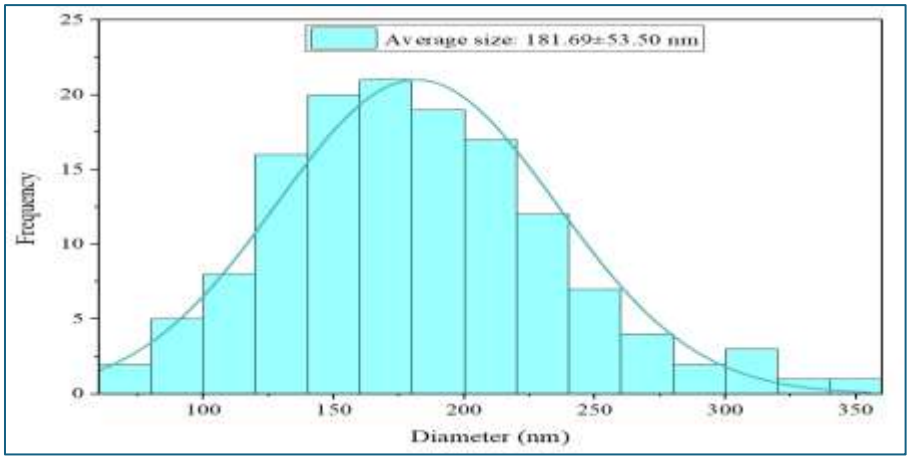

Figure 2: Particle size distribution of Chitosan-Lignin-IM nanocomposite, indicating nanoscale dimensions with most particles below 100 nm.

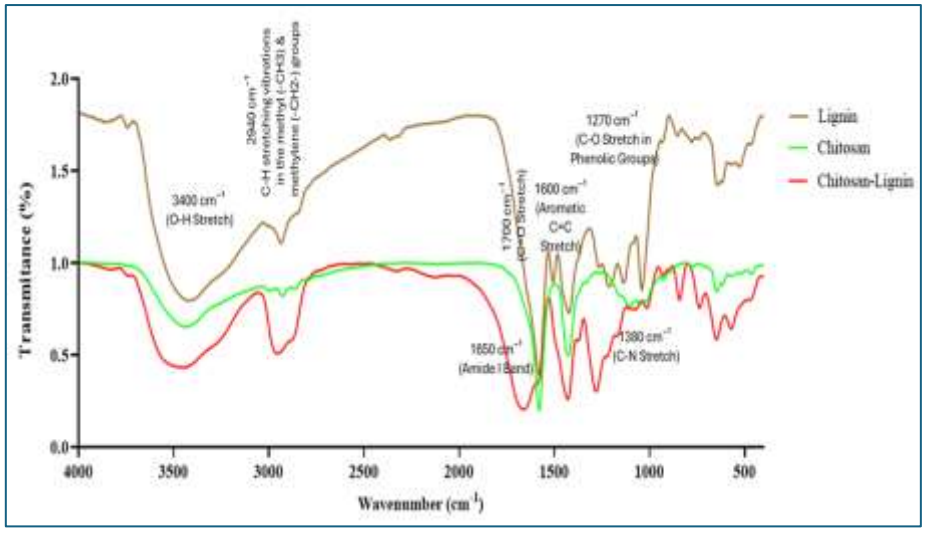

FT-IR Spectroscopic Analysis

FT-IR spectroscopy was employed to validate the chemical modifications and bonding interactions among chitosan, lignin, and the imidazole moiety. Figure 3 displays the comparative FT-IR spectra of pure chitosan, lignin, and the initial chitosan-lignin nanocomposite. In the chitosan spectrum, characteristic peaks at 3400 cm^{-1} and 1650 cm^{-1} correspond to –OH and $–NH_2$ stretching, respectively. Lignin showed distinct aromatic ring vibrations near 1510 cm^{-1} and C–O stretching around 1120 cm^{-1}. In the chitosan-lignin composite, shifts and overlaps in these peaks confirm hydrogen bonding and chemical interaction between the two polymers.

Figure 3: FT-IR spectra of chitosan, lignin, and chitosan-lignin nanocomposite. New peak patterns and shifts confirm molecular interaction and network formation.

Further insights are offered in Figure 4, which compares the FT-IR spectra of Chitosan-Lignin versus Chitosan-Lignin-IM. The imidazole-functionalized sample displays new bands near 1720 cm^{-1} and 1575 cm^{-1}, corresponding to C=O stretching and imidazole ring vibrations. These spectral features confirm the successful grafting of carboxylic imidazole onto the polymer backbone. The reduction in the –OH stretching intensity may indicate bonding interactions involving the imidazole moiety. Together, these results demonstrate chemical conjugation and structural enhancement of the nanocomposite.

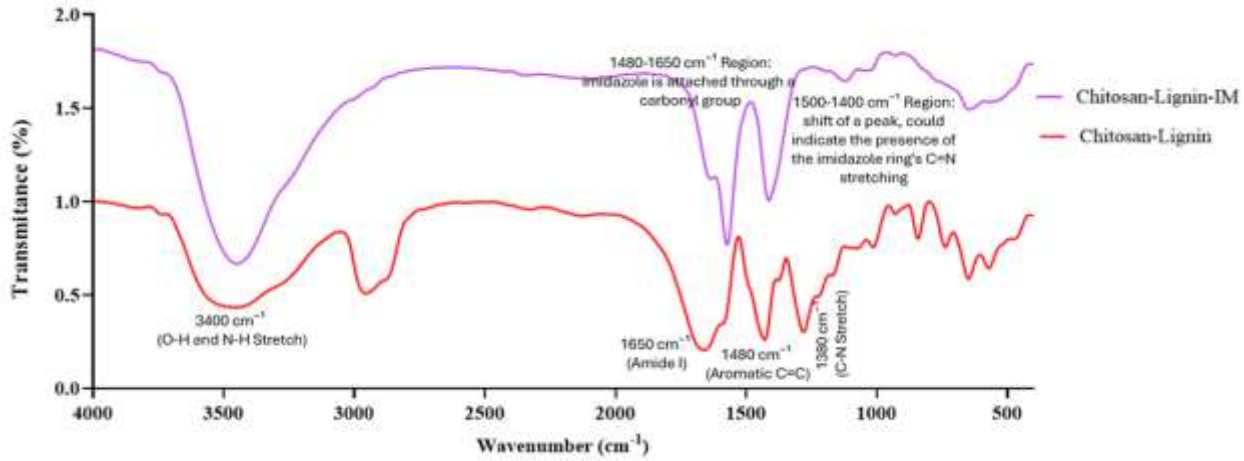

Figure 4: FT-IR spectra of Chitosan-Lignin and Chitosan-Lignin-IM nanocomposites, showing the emergence of new peaks from imidazole functional groups.

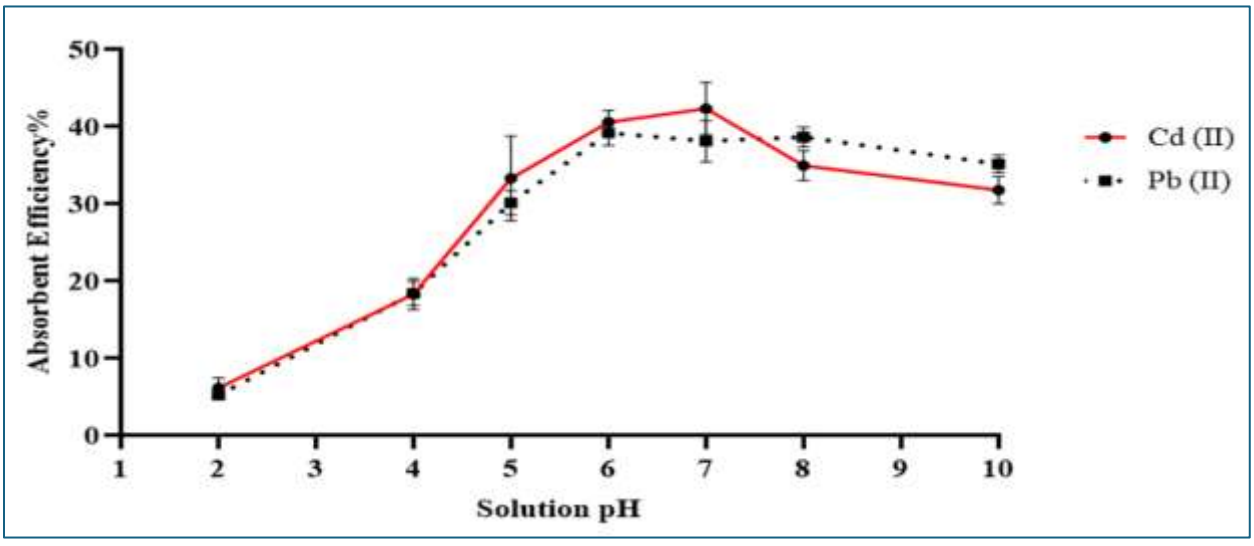

Adsorption Efficiency at Different pH Levels

The effect of pH on metal ion adsorption is summarized in Figure 5. The graph illustrates a clear increase in Cd^{2+} and Pb^{2+} removal efficiency as the pH rises from 2 to 7, with a sharp peak at neutral pH. At pH 6–7, over 90% of both metals were adsorbed by the nanocomposite. Below pH 4, adsorption was minimal due to proton competition and reduced ionization of active sites. At alkaline pH (above 8), precipitation of metal hydroxides likely interfered with adsorption processes, reducing effectiveness

Figure 5: Adsorption efficiency of Cd(II) and Pb(II) at different pH levels. Optimal adsorption observed at

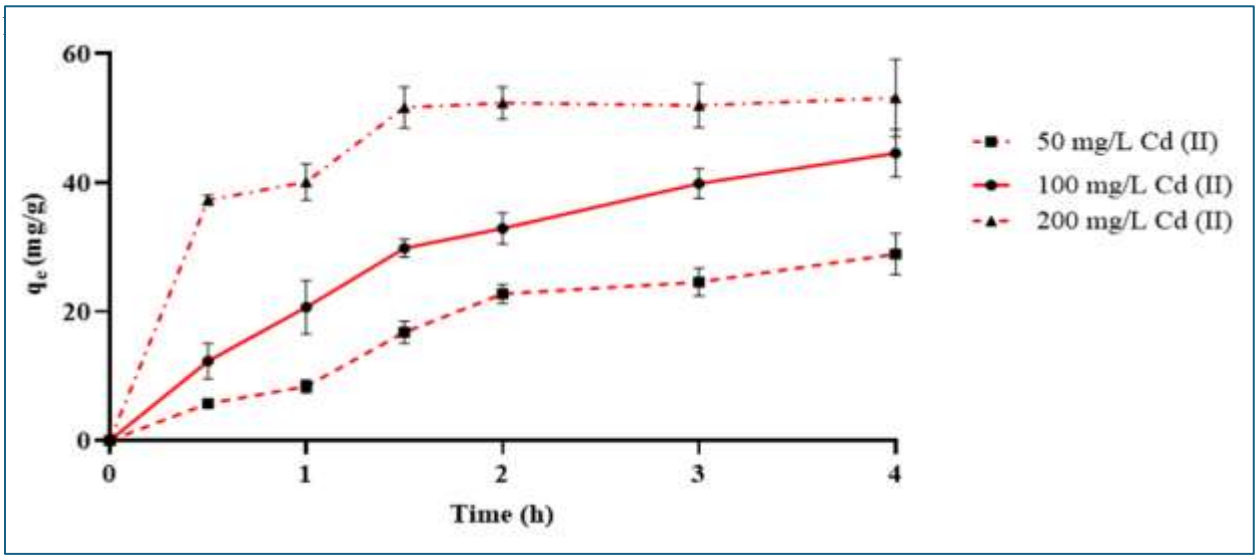

These findings indicate that pH is a crucial factor in optimizing adsorption. Neutral pH provides the best balance between ion availability and surface activity. The high performance at this range supports the potential use of the nanocomposite in natural and treated water systems, where pH commonly falls between 6 and 8. The imidazole groups may contribute to increased coordination with metal ions, further enhancing efficiency at favorable pH conditions.

Effect of Contact Time and Initial Concentration

Time-dependent adsorption studies for Cd^{2+} are displayed in Figure 6. At all initial concentrations, adsorption increased rapidly during the first 60–90 minutes, then slowed as equilibrium approached. The highest removal rate was achieved at 200 mg/L, with adsorption capacity reaching a plateau after approximately 2 hours. This behavior is consistent with surface saturation and suggests strong interaction between the active sites and metal ions.

Figure 6: Effect of contact time on the adsorption capacity of Chitosan-Lignin-IM nanocomposites for Cd(II) at different initial concentrations.

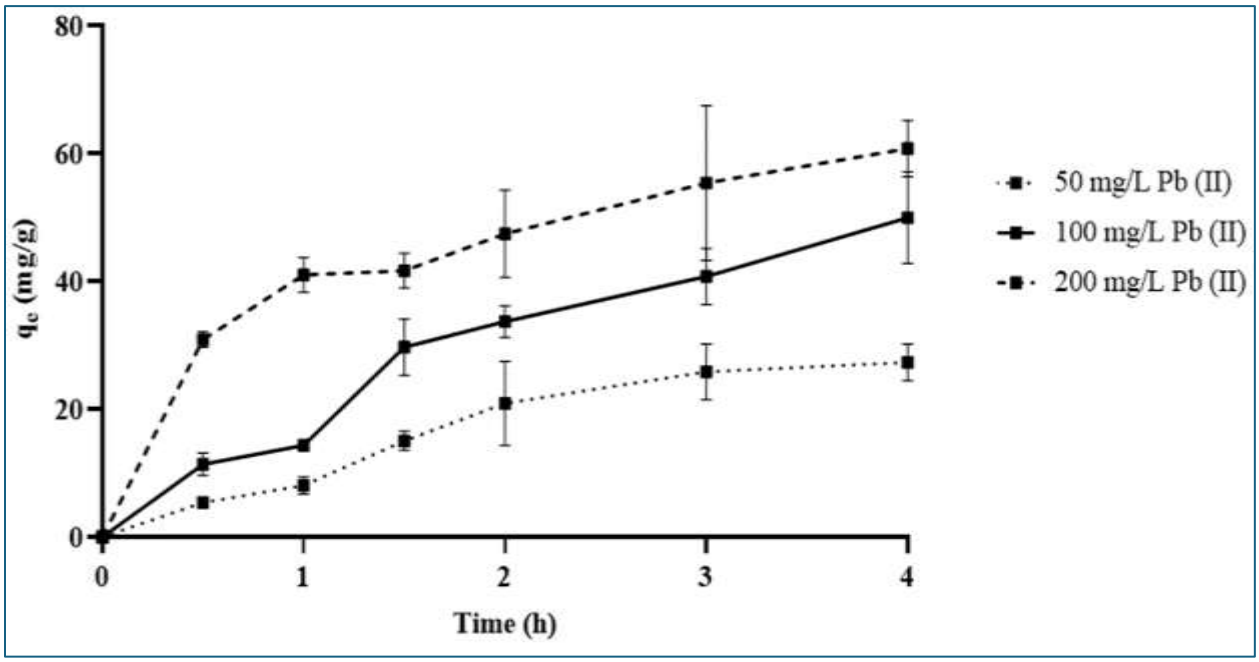

Figure 7 illustrates similar results for Pb^{2+} ions. The trend mirrors that of Cd^{2+}, with slightly higher adsorption capacities, reaching up to 165 mg/g. The saturation curves show that increasing the concentration leads to greater absolute uptake but reduced percentage removal, reflecting finite binding site availability. These findings reinforce the role of imidazole and amino groups in complexation and support the composite's effectiveness across a range of environmental metal concentrations.

Figure 7: Effect of contact time on the adsorption capacity of Chitosan-Lignin-IM nanocomposites for Pb(II) at different initial concentrations.

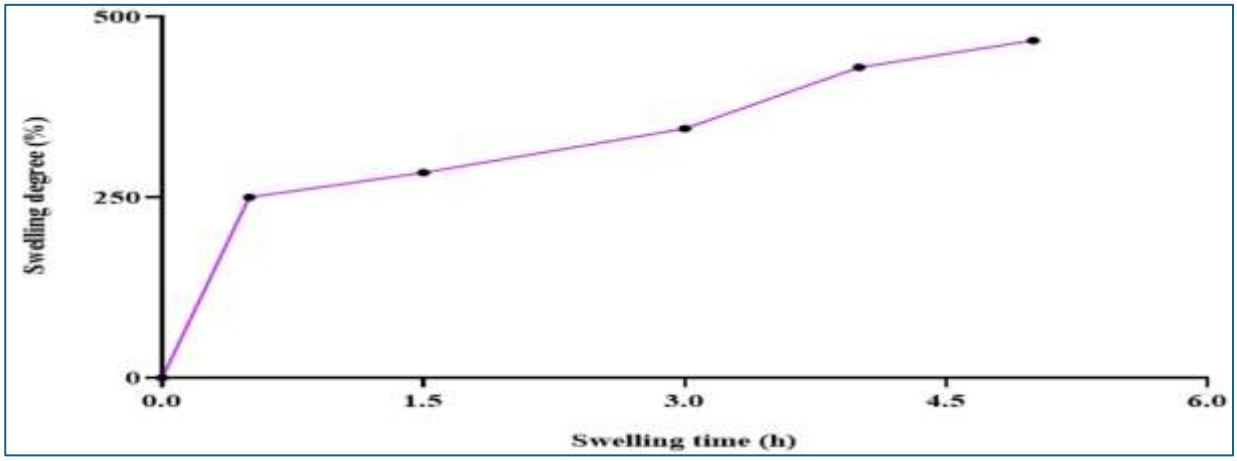

Swelling Behavior

The swelling kinetics of the Chitosan-Lignin-IM nanocomposite are presented in Figure 8 and detailed numerically in Table 1. The swelling degree increased steadily over time, beginning at 0% and reaching 467% after 5 hours. The sharp increase between 0.5 and 3 hours suggests rapid water uptake and pore expansion. This indicates good hydrogel-like properties, which help expose more internal binding sites for adsorption processes.

Figure 8: Swelling behavior of Chitosan-Lignin-IM nanocomposites over time in PBS at 37°C. Steady increase in swelling degree indicates hydrophilic and porous characteristics.

Table 1: Swelling Degree of Chitosan-Lignin-IM Nanocomposites Over Time

Swelling Degree (SD) (%)	Time (hours)
0	0
250	0.5
284	1.5
345	3
430	4
467	5

The high swelling behavior reflects the flexibility and porous nature of the polymer matrix. It also suggests good compatibility with aqueous environments. These traits improve diffusion and accessibility of metal ions to active sites. The controlled and gradual swelling also supports mechanical stability, which is essential for repeated use and practical filtration setups.

Rheological Analysis

The rheological profile of the nanocomposite is illustrated in Figure 10. The log–log plot of viscosity versus shear rate shows a marked decrease in viscosity with increasing shear rate, confirming shear-thinning behavior. This non-Newtonian response indicates that the material becomes easier to flow under mechanical stress, which is favorable for applications such as spraying, coating, or column packing.

Figure 10: Logarithmic plot of viscosity (Pa·s) versus shear rate (s^{-1}) for Chitosan-Lignin-IM nanocomposites. Shear-thinning behavior indicates non-Newtonian flow characteristics.

This flow behavior confirms the flexibility of the polymer chains and\

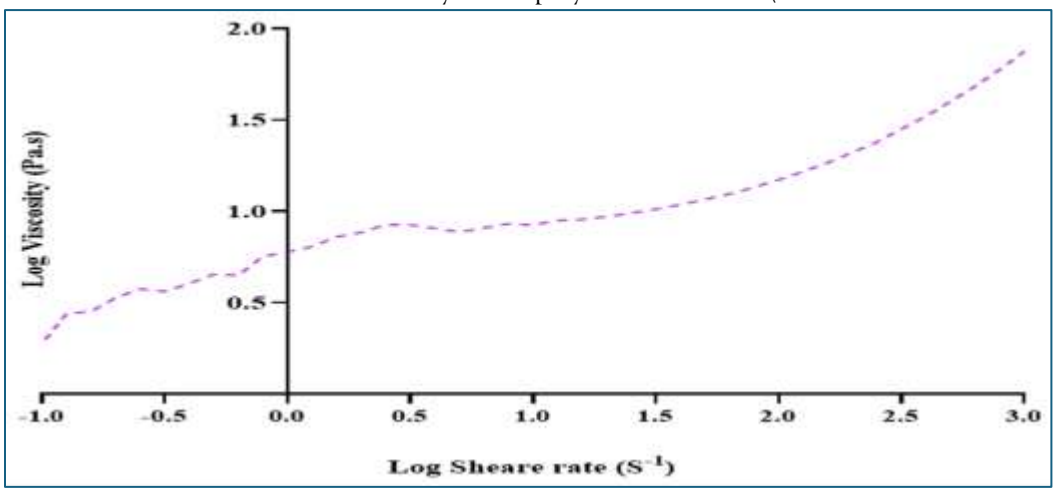

their ability to align under stress. It also implies that the composite can be processed easily in industrial systems without compromising structure. These results, combined with swelling and adsorption data, support the use of Chitosan-Lignin-IM as a versatile, eco-friendly adsorbent with excellent mechanical and functional performance.

DISCUSSION

The synthesis of Chitosan-Lignin-IM nanocomposites in this study showed that natural biopolymers can be successfully combined with imidazole groups. This created a hybrid material with strong ability to remove heavy metals from water. FESEM images revealed a clear nanostructure. The particles were evenly spread across the surface. This supports the idea of nanoscale integration. Ayanda et al. also found that better particle dispersion improves surface activity and pollutant binding. They explained this happens because of higher surface area and more active sites (16). FT-IR analysis further confirmed that imidazole groups were attached to the composite. This modification is important. It increases electron-donating properties and helps the material attract metal ions. A similar benefit was described by Boominathan and Sivaramakrishna. They showed that adding polar groups like imidazole to chitosan can enhance metal ion chelation and pollutant removal (20).The adsorption results in our study showed strong performance. The removal of Cd^{2+} and Pb^{2+} depended mostly on pH and the initial metal levels. The best results were seen when the pH was neutral or slightly acidic. This behavior is in agreement with findings from Qu and Luo, who demonstrated that chitosan-based hydrogel beads exhibit maximum metal ion uptake at pH 6–7 due to decreased competition with protons and increased surface deprotonation (17). In our study, the maximum adsorption capacity reached 165 mg/g for Pb^{2+}, a value that is comparable or superior to many reported biopolymer-based adsorbents. For instance, Grigoraş et al. reviewed chitosan–nanoparticle hydrogels for dye and ion removal and found that most systems plateaued at 100–150 mg/g, often requiring additional chemical activation (21). The Chitosan-Lignin-IM system in this study achieved similar or better performance without complex activation procedures, confirming its practical advantage.The swelling behavior of the nanocomposite was consistent with hydrogel characteristics, showing a gradual increase in swelling degree that peaked at 467% after 5 hours. Such behavior suggests a well-structured porous network, which facilitates diffusion and binding of metal ions. This is crucial for environmental applications where contact time is limited. Similar swelling profiles have been reported by Verma et al. in hydroxyapatite-based composites, highlighting that such materials benefit from both physical porosity and chemical interaction sites for pollutant capture (22). Moreover, the swelling performance seen here did not compromise the structural integrity of the films, which

contrasts with some synthetic hydrogels that degrade under extended hydration. The combination of stability and hydrophilicity in this study demonstrates the synergy between chitosan and lignin, as discussed by Kanaoujiya et al., who described biopolymer composites as superior in structural resilience compared to traditional gels (18).The rheological analysis confirmed the shear-thinning behavior of the Chitosan-Lignin-IM nanocomposite, which is beneficial for environmental systems that involve flow or dynamic filtration. Shear-thinning properties enable easier application through pumps or columns while maintaining structural coherence under low-shear conditions. This performance is consistent with the behavior of GO/TiO_2-based nanocomposites described by Kong et al., where high viscosity at rest combined with flow reduction under shear was linked to processability and efficiency in wastewater systems (19). Additionally, comparisons can be drawn with activated carbon–based nanocomposites, where similar structural modifications yielded better pollutant interactions and longer operational life in filtration devices (27). Altogether, the data suggest that Chitosan-Lignin-IM nanocomposites provide a balanced combination of mechanical, chemical, and functional properties that support their use in real-world remediation systems.

CONCLUSION

In this study, Chitosan-Lignin-IM nanocomposites were successfully synthesized and evaluated for their ability to remove Cd^{2+} and Pb^{2+} ions from aqueous solutions. The material demonstrated excellent adsorption capacity, reaching up to 165 mg/g for Pb^{2+}, with optimal performance at neutral pH. Structural characterization confirmed the formation of a stable, functional nanocomposite, while swelling and rheological analyses revealed favorable water absorption and shear-thinning properties. Compared to similar systems in recent literature, this composite exhibited strong efficiency without requiring complex activation steps. Its eco-friendly composition, ease of preparation, and high removal efficiency make it a promising candidate for sustainable heavy metal remediation in water treatment applications.

REFERENCES

1. Goci MC, Leudjo Taka A, Martin L, Klink MJ. Chitosan-Based Polymer Nanocomposites for Environmental Remediation of Mercury Pollution. Polymers (Basel). 2023 Jan 17;15(3):482. doi: 10.3390/polym15030482.
2. Sajjadi M, Ahmadpoor F, Nasrollahzadeh M, Ghafuri H. Lignin-derived (nano)materials for environmental pollution remediation: Current challenges and future perspectives. Int J Biol Macromol. 2021 May 1;178:394-423. doi: 10.1016/j.ijbiomac.2021.02.165.
3. Wang X, Tarahomi M, Sheibani R, Xia C, Wang W. Progresses in lignin, cellulose, starch, chitosan, chitin, alginate, and gum/carbon nanotube (nano)composites for environmental applications: A review. Int J Biol Macromol. 2023 Jun 30;241:124472. doi: 10.1016/j.ijbiomac.2023.124472.
4. Rostami MS, Khodaei MM. Recent advances in chitosan-based nanocomposites for adsorption and removal of heavy metal ions. Int J Biol Macromol. 2024 Jun;270(Pt 2):132386. doi: 10.1016/j.ijbiomac.2024.132386.
5. Detellier C. Functional Kaolinite. Chem Rec. 2018 Jul;18(7-8):868-877. doi: 10.1002/tcr.201700072.
6. Bhatt P, Joshi S, Urper Bayram GM, Khati P, Simsek H. Developments and application of chitosan-based adsorbents for wastewater treatments. Environ Res. 2023 Jun 1;226:115530. doi: 10.1016/j.envres.2023.115530.
7. Iftekhar S, Deb A, Heidari G, Sillanpää M, Lehto VP, Doshi B, et al. A review on the effectiveness of nanocomposites for the treatment and recovery of oil spill. Environ Sci Pollut Res Int. 2023 Feb;30(7):16947-16983. doi: 10.1007/s11356-022-25102-1.
8. Amari A, Alzahrani FM, Katubi KM, Alsaiari SN, Tahoon MA, Ben Rebah F. Clay-Polymer Nanocomposites: Preparations and Utilization for Pollutants Removal. Materials (Basel). 2021 Mar 11;14(6):1365. doi: 10.3390/ma14061365.
9. Bruckmann FS, Schnorr C, Oviedo LR, Knani S, Silva LFO, Silva WL, et al. Adsorption and Photocatalytic Degradation of Pesticides into Nanocomposites: A Review. Molecules. 2022 Sep 23;27(19):6261. doi: 10.3390/molecules27196261.
10. Memisoglu G, Murugesan RC, Zubia J, Rozhin AG. Graphene Nanocomposite Membranes: Fabrication and Water Treatment Applications. Membranes (Basel). 2023 Jan 22;13(2):145. doi: 10.3390/membranes13020145.
11. Khan MI, Almesfer MK, Elkhaleefa A, Shigidi I, Shamim MZ, Ali IH, Rehan M. Conductive Polymers and Their Nanocomposites as Adsorbents in Environmental Applications. Polymers (Basel). 2021 Nov 4;13(21):3810. doi: 10.3390/polym13213810.
12. Rando G, Sfameni S, Galletta M, Drommi D, Cappello S, Plutino MR. Functional Nanohybrids and Nanocomposites Development for the Removal of Environmental Pollutants and Bioremediation. Molecules. 2022 Jul 29;27(15):4856. doi: 10.3390/molecules27154856.
13. Tran TV, Nguyen DTC, Kumar PS, Din ATM, Jalil AA, Vo DN. Green synthesis of ZrO_2 nanoparticles and nanocomposites for biomedical and environmental applications: a review. Environ Chem Lett. 2022;20(2):1309-1331. doi: 10.1007/s10311-021-01367-9.

14. Harun-Ur-Rashid M, Imran AB, Susan MABH. Green Polymer Nanocomposites in Automotive and Packaging Industries. Curr Pharm Biotechnol. 2023;24(1):145-163. doi: 10.2174/1389201023666220506111027.
15. Wang H, Ma J, Zhang J, Feng Y, Vijjapu MT, Yuvaraja S, et al. Gas sensing materials roadmap. J Phys Condens Matter. 2021 Jun 11;33(30). doi: 10.1088/1361-648X/abf477.
16. Ayanda OS, Quadri RO, Adewuyi SO, Mmuoegbulam AO, Okezie O, Mohammed SE, et al. Multidimensional applications and potential health implications of nanocomposites. J Water Health. 2023 Aug;21(8):1110-1142. doi: 10.2166/wh.2023.141. PMID: 37632385.
17. Qu B, Luo Y. Chitosan-based hydrogel beads: Preparations, modifications and applications in food and agriculture sectors - A review. Int J Biol Macromol. 2020 Jun 1;152:437-448. doi: 10.1016/j.ijbiomac.2020.02.240. PMID: 32097742.
18. Kanaoujiya R, Saroj SK, Rajput VD, Alimuddin, Srivastava S, Minkina T, et al. Emerging application of nanotechnology for mankind. Emergent Mater. 2023;6(2):439-452. doi: 10.1007/s42247-023-00461-8. PMID: 36743193.
19. Kong EDH, Chau JHF, Lai CW, Khe CS, Sharma G, Kumar A, et al. GO/TiO(2)-Related Nanocomposites as Photocatalysts for Pollutant Removal in Wastewater Treatment. Nanomaterials (Basel). 2022 Oct 10;12(19):3536. doi: 10.3390/nano12193536. PMID: 36234665.
20. Boominathan T, Sivaramakrishna A. Recent Advances in the Synthesis, Properties, and Applications of Modified Chitosan Derivatives: Challenges and Opportunities. Top Curr Chem (Cham). 2021 Apr 8;379(3):19. doi: 10.1007/s41061-021-00331-z. PMID: 33829312.
21. Grigoraş CG, Simion AI, Drob C. Hydrogels Based on Chitosan and Nanoparticles and Their Suitability for Dyes Adsorption from Aqueous Media: Assessment of the Last-Decade Progresses. Gels. 2024 Mar 21;10(3):211. doi: 10.3390/gels10030211. PMID: 38534629.
22. Verma R, Mishra SR, Gadore V, Ahmaruzzaman M. Hydroxyapatite-based composites: Excellent materials for environmental remediation and biomedical applications. Adv Colloid Interface Sci. 2023 May;315:102890. doi: 10.1016/j.cis.2023.102890. PMID: 37054653.